
XMM-Newton Spectrum of the magnetar CXOU J171405.7–381031

Haruka Watanabe,¹ Aya Bamba,^{2,3} Shinpei Shibata,⁴ and Eri Watanabe¹

¹School of Science and Technology, Yamagata University, 1-4-12 Kojirakawa, Yamagata 990-8560, Japan

²Department of Physics, The University of Tokyo, 7-3-1 Hongo, Bunkyo-ku, Tokyo 113-0033, Japan

³Research Center for the Early Universe, School of Science, The University of Tokyo, 7-3-1 Hongo, Bunkyo-ku, Tokyo 113-0033, Japan

⁴Department of Physics, Yamagata University, 1-4-12 Kojirakawa, Yamagata 990-8560, Japan

*E-mail: shibata@sci.kj.yamagata-u.ac.jp

Received (reception date); Accepted (acceptation date)

Abstract

We observe the magnetar CXOU J171405.7–381031 with XMM-Newton and obtain the most reliable X-ray spectral parameters for this magnetar. After removing the flux from the surrounding supernova remnant CTB 37B, the radiation of CXOU J171405.7–381031 is best described by a two-component model, consisting of a blackbody and power law. We obtain a blackbody temperature of $0.58^{+0.03}_{-0.03}$ keV, photon index of $2.15^{+0.62}_{-0.68}$, and unabsorbed 2–10 keV band flux of $2.33^{+0.02}_{-0.02} \times 10^{-12}$ erg cm^{−2} s^{−1}. These new parameters enable us to compare CXOU J171405.7–381031 with other magnetars, and it is found that the luminosity, temperature and the photon index of CXOU J171405.7–381031 are aligned with the known trend among the magnetar population with a slightly higher temperature, which could be caused by its young age. All the magnetars with a spin-down age of less than 1 kyr show time variation or bursts except for CXOU J171405.7–381031. We explore the time variability for ten observations in between 2006 and 2015, but there is no variation larger than $\sim 10\%$.

Key words: stars: magnetars — stars: individual (CXOU J171405.7–381031) — X-rays: stars

1 Introduction

Magnetars are strongly magnetized neutron stars. Their magnetic fields, which are inferred from the rotation period and its time derivative, typically exceed the quantum critical field strength $B_Q = m^2 c^3 / \hbar e = 4.4 \times 10^{13}$ G. Most of their luminosity is in the X-ray bands, and the origin of the radiation is believed to be the decay of the strong magnetic field, although its mechanism and radiation process are not well understood (for reviews, see Turolla et al. 2015, Kaspi & Beloborodov 2017). X-ray spectra of magnetars in quiescence are generally multi-component; therefore, it is important to obtain precise spectra to distinguish the components and clarify the emission mechanism. The standard spectral model for magnetars is a blackbody plus power law model (BB+PL) in the 0.5–10 keV bands, although two blackbody models (2BB) are sometimes used. The Comptonized blackbody model (CBB) or an appropriate neutron-star atmosphere model are also sometimes useful. The spectrum turns upward in the higher energy bands $\gtrsim 10$ keV (Kuiper et al. 2004), so X-ray radiation from magnetars is generally decomposed into a soft thermal component and a hard non-thermal component. Enoto et al. (2010) reported that the ratio of the soft thermal flux and the hard non-thermal flux, $F(15 - 60 \text{ keV})/F(1 - 10 \text{ keV})$, is negatively correlated with the spin-down age and positively correlated with the dipole field strength. More importantly, the magnetars show time variability on various time scales from milliseconds to seconds (outbursts) and also on longer time scales (e.g., Kaspi & Beloborodov 2017). In this paper, we report detailed spectroscopy of the magnetar CXOU J171405.7–381031 with XMM-Newton and time variability over a decade.

CXOU J171405.7–381031 was found as an X-ray point source associated with the shell-type supernova remnant (SNR) CTB 37B (Aharonian et al. 2008) in the Chandra follow-up observation for the TeV source HESS J1713–38 (Aharonian et al. 2006). The SNR is also detected in the GeV band with Fermi LAT (Xin et al. 2016). Sato et al. (2010) and Halpern & Gotthelf (2010b) found the pulse period and its time derivative, and they concluded that CXOU J171405.7–381031 is a magnetar. The period and its time derivative are $P = 3.825$ s and $\dot{P} = 6.4 \times 10^{-11} \text{ s s}^{-1}$, respectively, which provide the spin-down luminosity of $L_{\text{rot}} = 4.5 \times 10^{34} \text{ erg s}^{-1}$, a dipole field of $B_d = 5.0 \times 10^{14}$ G and a characteristic age of $\tau = 0.95$ kyr. These parameters make CXOU J171405.7–381031 the fourth youngest magnetar known and the fourth strongest magnetic field known. The distance is estimated to be ~ 13.2 kpc (Tian & Leahy 2012).

The spectrum of CXOU J171405.7–381031 was not well determined by the previous Chandra observation made on 25 January 2009 and 30 January 2010 (Halpern & Gotthelf 2010a, 2010b). Sato et al. (2010) observed CXOU J171405.7–381031 with XMM-Newton on 17–18 March 2010 and analysed only the pn data. They fitted the data by a power law model only. In this paper, we use MOS data and pn data and apply multi-component spectral models that are standard for magnetars.

2 Analysis

2.1 Observation and data reduction

CXOU J171405.7–381031 was observed with XMM-Newton from 13:16:16, 17 2010 March to 23:06:33, 18 March 2010 (ObsID = 0606020101). For the spectral analysis we used data from the European Photon Imaging Camera (EPIC) instruments: MOS (Tumer et al. 2001) and pn (Strüder et al. 2001). Both the MOS and the pn instruments were configured in full-frame mode, with a medium filter.

Data reduction was performed with SAS version 16.1.0 and the SAS guide. The data reduction was done with SAS version 16.1.0 and the SAS guide. We filtered out background flare times for rates in the 10–12 keV band higher than 0.35 cnts s^{-1} , resulting in a total exposure of 100.4 ks for MOS1, 100.7 ks for MOS2 and 46.8 ks for pn. For the following analysis, we used *heasoft* 6.18 package. We also used Chandra data and short-exposure XMM-Newton data for the flux monitoring. Chandra observed CXOU J171405.7–381031 four times with ACIS-S in the continuous clocking mode and once with ACIS-I in Timed Exposure modes in very faint telemetry format. The data reduction was done with CIAO version 4.9, and the total exposure was ~ 20 ks for each data set (Table 1). After 2010, XMM-Newton observed three times in the small window mode with the exposure time of ~ 20 ks, and these data are used for the flux monitoring. The details of the observations are summarized in Table 1.

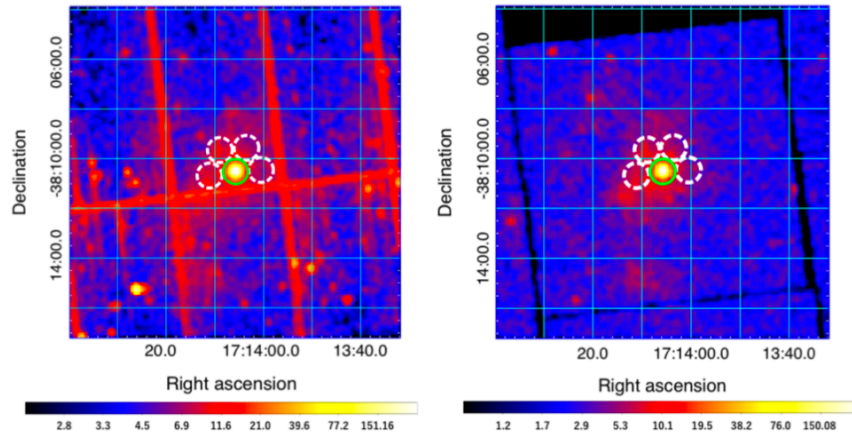
2.2 Spectral analysis

Figure 1 shows the MOS and pn images of the SNR CTB 37B region. CXOU J171405.7–381031 is detected as a bright point source near the center of CTB 37B. For our spectral analysis, we took the source region as a circular region centered at $\ell = 348^\circ 40' 51''$, $b = 0^\circ 22' 15''.820$ with a radius of $30''$ (Sato et al. 2010).

CXOU J171405.7–381031 is located within the SNR, so the SNR counts must be subtracted from the source counts. We took background regions near the source, namely the four circular regions with the same radius as the source region, indicated by the

Table 1. Observation log of CXOU J171405.7–381031

Date (YYYY/MM/DD)	Satellite	ObsID	Exposure (ks)
2010/03/17	XMM-Newton	0606020101	100 (MOS) 45 (pn)
2007/02/02	Chandra	6692	25 (ACIS-I)
2009/01/25	Chandra	10113	30 (ACIS-S)
2010/01/30	Chandra	11233	26 (ACIS-S)
2012/07/16	Chandra	13749	20 (ACIS-S)
2015/10/13	Chandra	16763	20 (ACIS-S)
2012/03/13	XMM-Newton	0670330101	13 (MOS)
2016/09/23	XMM-Newton	0790870201	29 (MOS)
2017/02/22	XMM-Newton	0790870301	22 (MOS)

**Fig. 1.** XMM-Newton MOS (right panel) and pn (left panel) images of the CTB 37B region in the 1–10 keV band. The source regions for CXOU J171405.7–381031 are indicated by the green circles, and the background regions are indicated by the dashed white circles.

dashed circles in Figure 1. For MOS and pn, the background regions were set to avoid the edges of the CCD chips. We used these four regions together to obtain the background-subtracted source counts. The background contribution is $\sim 0.08\%$ of the source counts in the 1–10 keV band.

An acceptable spectral fit was not obtained with a single blackbody or a single power law. Two-component models, either the 2BB model or the BB+PL model, generally give a good fit for magnetars. The 2BB model with interstellar absorption (phabs: Balucinska-Church & McCammon 1992) gave a reasonably good fit to the present data set with $\chi^2/\text{d.o.f} = 332.39/306$. The hydrogen column density, lower and higher blackbody temperatures, and unabsorbed flux are $n_H = 2.50^{+0.11}_{-0.10} \times 10^{22} \text{ cm}^{-2}$, $kT_1 = 0.61^{+0.02}_{-0.02} \text{ keV}$, $kT_2 = 2.10^{+0.50}_{-0.33} \text{ keV}$, and $F_x = 2.21^{+0.02}_{-0.02} \times 10^{-12} \text{ erg cm}^{-2} \text{ s}^{-1}$ in the 2–10 keV band, respectively. The spectral parameters are summarized in Table 2. The errors are given at the 90% confidence level, and this is the same throughout this paper.

We also obtained a reasonably good fit by using the absorbed BB+PL model, where the same absorption model (phabs) is used. The chi squared value was $\chi^2/\text{d.o.f} = 325.40/306$, which was slightly better than that of the 2BB fit. Figure 2 shows the background-subtracted spectrum of CXOU J171405.7–381031 together with the fitted model spectrum and the residuals. MOS1, MOS2 and pn data were jointly fitted by a single model. The hydrogen column density is $n_H = 2.84^{+0.43}_{-0.28} \times 10^{22} \text{ cm}^{-2}$, and the blackbody temperature, photon index and unabsorbed flux are $kT = 0.58^{+0.03}_{-0.03} \text{ keV}$, $\Gamma = 2.15^{+0.62}_{-0.68}$, $F_x = 2.33^{+0.02}_{-0.02} \times 10^{-12} \text{ erg cm}^{-2} \text{ s}^{-1}$ in the 2–10 keV band, respectively. The results are summarized in Table 2.

We evaluated systematic uncertainties due to inhomogeneous background emission from the SNR. We subtracted each of the four background counts from the source counts to examine how the spectral parameters vary. We find that the systematic errors for the obtained n_H , Γ and kT for the BB+PL model are $0.45 \times 10^{22} \text{ cm}^{-2}$, 0.64, 0.037 keV, at the 90% confidence level, which are 130%, 98% and 130% of the statistical error, respectively. Thus the systematic error due to the inhomogeneity of the SNR was comparable to the statistical error.

In the magnetosphere of persistent magnetars, high-energy particles are thought to be supplied continuously into magnetic loops, so the hard component can be interpreted as a Comptonized tail of the blackbody radiation by these high-energy particles (Turolla et

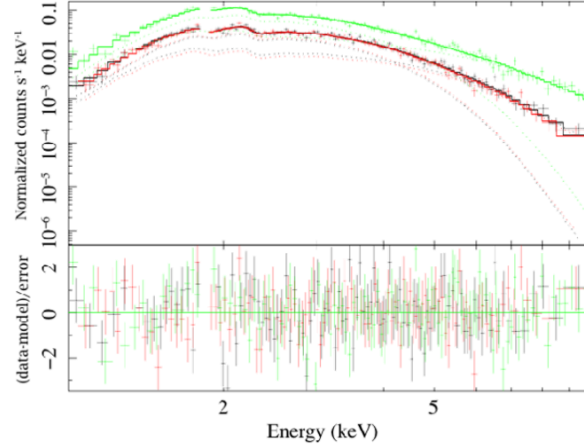


Fig. 2. XMM-Newton MOS and pn spectra of CXOU J171405.7–381031. The top panel shows the data (crosses) and best fit model (solid line) for the parameter given in Table 2. The spectral components are shown by the dashed lines. The data for MOS1, MOS2 and pn are shown in black, red and green, respectively. The bottom panel shows the residuals.

Table 2. Spectral fits to CXOU J171405.7–381031

Parameter	2BB	BB+PL	CBB
chi-Squared/d.o.f	332.39/306	325.40/306	329.67/309
Hydrogen column density*1	$2.50^{+0.11}_{-0.10}$	$2.84^{+0.43}_{-0.28}$	$2.63^{+0.10}_{-0.10}$
kT_1 (keV)	$0.61^{+0.02}_{-0.02}$	$0.58^{+0.03}_{-0.03}$	$0.56^{+0.02}_{-0.02}$
R_1 (km)	$1.82^{+0.01}_{-0.01}$	$1.83^{+0.01}_{-0.02}$...
kT_2 (keV)	$2.10^{+0.50}_{-0.33}$
R_2 (km)	$0.084^{+0.002}_{-0.001}$
Photon index	...	$2.15^{+0.62}_{-0.68}$...
Optical depth	$0.43^{+0.02}_{-0.02}$
Observed flux*2	$1.58^{+0.02}_{-0.02}$	$1.58^{+0.02}_{-0.02}$	$1.58^{+0.02}_{-0.02}$
Intrinsic flux*2	$2.21^{+0.02}_{-0.02}$	$2.33^{+0.02}_{-0.02}$	$2.25^{+0.02}_{-0.02}$

*1 in units of 10^{22} cm^{-2}

*2 in units of $10^{-12} \text{ erg cm}^{-2} \text{ s}^{-1}$ in the 2–10 keV band

al., 2015). We also attempted the fitting with the CCB model. The results are summarised in Table 2. The electron temperature was assumed to be 50 keV and 100 keV, and both gave a good fit with similar blackbody temperatures. In this case, an additional power component was not needed. Notably, the standard two-component model and CBB model give similar temperatures. The best fit was given by BB+PL, followed by CB and 2BB.

We explored the long-term flux variation for CXOU J171405.7–381031 because this class of magnetars, which has a characteristic age smaller than 1 kyr shows burst activity or variability.

We reanalyzed the previous Chandra observations and XMM-Newton observations using the present BB+PL spectral parameters, which were fixed except for the normalization, to determine the flux variability. The χ^2 values were stable and acceptable for all the data, and the flux variability results are summarized in Table 3 and Figure 3. We found no significant variation in the flux for about a decade. The mean value of the flux in the 2–10 keV band was $1.45 \times 10^{-12} \text{ erg cm}^{-2} \text{ s}^{-1}$ with the standard deviation of $0.14 \times 10^{-12} \text{ erg cm}^{-2} \text{ s}^{-1}$ (9.7% of the mean).

3 Discussion

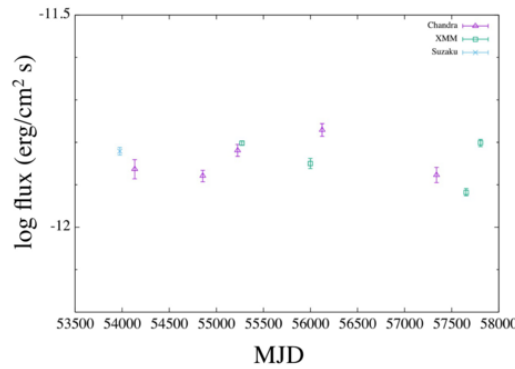
In this paper, we have obtained the most reliable spectral parameters for CXOU J171405.7–381031 so far by using XMM-Newton. In the previous Chandra ACIS-I/TE mode observation on 25 January 2009 the data showed a rising spectrum above $> 6 \text{ keV}$, such that the 2BB fit gave an unphysical high temperature and the BB+PL fit gave a photon index of -2 , which is unusual (Halpern & Gotthelf, 2010a). These high-energy events disappear in the Chandra CC mode observation on 30 January 2010 (Halpern & Gotthelf 2010b). They argued that the pulsar was dithered into the gap between CCD's. Thus, the spectral fit for CXOU J171405.7–381031

Table 3. Long term variation of CXOU J171405.7–381031

Date	flux*1(2-10keV)	Model	Mission	Refs
2006/08/27-29	$1.510^{+0.030}_{-0.030}$	PL	Suzaku	1
2007/02/02	$1.371^{+0.072}_{-0.072}$	BB+PL	Chandra	2
2009/01/25	$1.320^{+0.041}_{-0.041}$	BB+PL	Chandra	2
2010/01/30	$1.517^{+0.049}_{-0.049}$	BB+PL	Chandra	2
2010/03/17-18	$1.578^{+0.017}_{-0.017}$	BB+PL	XMM	2
2012/01/16	$1.695^{+0.060}_{-0.059}$	BB+PL	Chandra	2
2012/03/13	$1.414^{+0.040}_{-0.039}$	BB+PL	XMM	2
2015/11/13	$1.329^{+0.055}_{-0.055}$	BB+PL	Chandra	2
2016/09/23	$1.209^{+0.023}_{-0.023}$	BB+PL	XMM	2
2017/02/22	$1.581^{+0.031}_{-0.031}$	BB+PL	XMM	2

*1 absorbed flux in units of $10^{-12} \text{ erg cm}^{-2} \text{ s}^{-1}$

References, 1: Nakamura et al.(2009), 2: this work.

**Fig. 3.** The long term history of the absorbed flux of CXOU J171405.7–381031 in the 2 – 10 keV bands.

was uncertain. We reanalyzed the Chandra data in the previous section and find that our 2BB parameters also give a good fit with $\chi^2/\text{dof} = 131.86/135$. The Chandra result (Halpern & Gotthelf, 2010b) gave a ~ 1.4 times higher T_1 and a ~ 1.5 times larger hydrogen column density than the present XMM result. The difference is caused by how the high energy part is fit, and the Chandra data does not give enough statistics in the high energy part. The XMM-Newton observation on 17–18 March 2009 was analyzed using only the pn data with a single PL model (Sato et al., 2010). In this paper, we analyze both MOS and pn data to give the spectral parameters for the two-component models that are commonly used for magnetars.

In the case of the 2BB fit, the ratio of the two temperatures of each components shows a correlation over a large number of both persistent and transient magnetars, as seen in Fig. 3 of Nakagawa et al. (2009), namely, $kT_2/kT_1 = 2.7 \pm 1.1$. The present value of 3.4 ($= 2.10 \text{ keV}/0.61 \text{ keV}$) follows this correlation. They suggested that the ratio of the emitting area is $R_2^2/R_1^2 \approx 0.01$, whereas we find $R_2^2/R_1^2 = 0.02$, and this is again along the general trend in the scatter (see also Fig. 3 of Nakagawa et al., 2009).

As shown in the previous section, the BB+PL model gives the best fit giving the X-ray luminosity in the 2 – 10 keV band as $L_x = 4.9 \times 10^{34} d_{13.2}^2 \text{ erg s}^{-1}$, which exceeds the spin-down power and is a typical value for persistent magnetars. The blackbody component gives an intrinsic bolometric flux of $2.34 \times 10^{-12} \text{ erg cm}^{-2} \text{ s}^{-1}$ and an emitting radius of $1.8 d_{13.2} \text{ km}$ at a distance of 13.2 kpc, to which the normalized distance, $d_{13.2}$, refers. For the persistent magnetars, a positive correlation between the blackbody temperature and the dipole field has been suggested (Pons et al., 2007; Enoto et al. 2017). Although it was also suggested that the correlation is not solid due to a large scatter (Zhu et al., 2011), the scatter seems natural because the surface magnetic field has multi-polar components. In other words, the magnetic field is composed of many magnetic loops, and therefore the dipole field does not always represent the surface magnetic field but would still be related to the surface field. Figure 4 shows the scatter plot of the blackbody temperature and the dipole field strength obtained by Enoto et al. (2017), showing a positive correlation. Our result for CXOU J171405.7–381031 follows this trend, but it is at a higher position than the general trend. This may be because CXOU J171405.7–381031 is the fourth youngest magnetar known.

The hard power law component of the magnetar spectrum extends to the soft gamma-ray bands with photon a index between 0 to

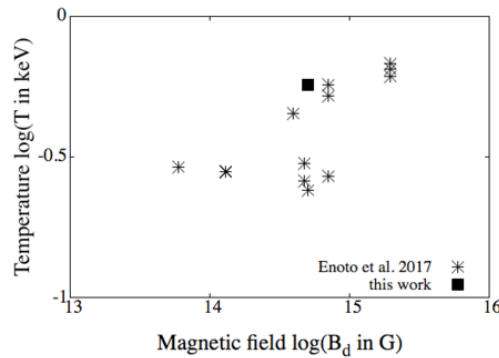


Fig. 4. kT versus B_d for the persistent emission of the magnetars (Enoto 2017) and the present result for CXOU J171405.7–381031.

2. The photon index shows a positive correlation with the magnetic field (Enoto et al., 2010; Kaspi & Boydstun, 2010). We obtained a photon index of 1.9 for CXOU J171405.7–381031, which follows this correlation. However, the hard power component becomes dominant beyond ~ 10 keV, which is outside the present observations. Therefore, the photon index obtained in this work is not that of the hard power law component. In fact, the CBB model does not require the power law component. Future observations above 10 keV are required.

The magnetar population consists of persistent and transient sources. The typical luminosity of the persistent sources is $10^{33} - 10^{35} \text{ erg s}^{-1}$. The transient sources brighten to this range of luminosity in burst phases, but generally they dim to levels that cannot be observed with the current instruments. The origin of the difference between persistent and transient sources is unknown. In this work, we did not find any significant change in luminosity for CXOU J171405.7–381031. However, the four magnetars that have characteristic ages of less than 1 kyr, SGR 1806–20, 1E 1841–045, SGR 1900+14, and 1E 1547.0–5408, all show outbursts (Coti Zelati et al., 2018). Consequently, we still need to monitor this object.

Acknowledgments

We acknowledge support from JSPS/MEXT KAKENHI grant numbers 18H01246 (SS), 15K051017 (AB) and JP18H05459 (AB). This work was also supported by the Grant-in-Aid for Scientific Research on Innovative Areas “Toward new frontiers : Encounter and synergy of state-of-the-art astronomical detectors and exotic quantum beams” (AB).

References

- Aharonian, F., Akhperjanian, A. G., Barres de Almeida, U., et al. 2008, *A&A*, 486, 829
- Balucinska-Church, M., & McCammon, D. 1992, *ApJ*, 400, 699
- Coti Zelati, F., Rea, N., Pons, J. A., Campana, S., & Esposito, P. 2018, *MNRAS*, 474, 961
- Enoto, T., Nakazawa, K., Makishima, K., Rea, N., Hurley, K., & Shibata, S. 2010, *ApJL*, 722, L162
- Enoto, T., Shibata, S., Kitaguchi, T., et al. 2017, *ApJS*, 231, 8
- Halpern, J. P., & Gotthelf, E. V. 2010a, *ApJ*, 710, 941
- Halpern, J. P., & Gotthelf, E. V. 2010b, *ApJ*, 725, 1384
- Kaspi, V. M., & Beloborodov, A. M. 2017, *ARA&A*, 55, 261
- Kaspi, V. M., & Boydstun, K. 2010, *ApJL*, 710, L115
- Kuiper, L., Hermesen, W., & Mendez, M. 2004, *ApJ*, 613, 1173
- Nakagawa, Y. E., Yoshida, A., Yamaoka, K., & Shibasaki, N. 2009, *PASJ*, 61, 109
- Nakamura, R., Bamba, A., Ishida, M., et al. 2009, *PASJ*, 61, S197
- Pons, J. A., Link, B., Miralles, J. A., & Geppert, U. 2007, *Physical Review Letters*, 98, 071101
- Sato, T., Bamba, A., Nakamura, R., & Ishida, M. 2010, *PASJ*, 62, L33
- Turolla, R., Zane, S., & Watts, A. L. 2015, *Reports on Progress in Physics*, 78, 116901
- Xin, Y.-L., Liang, Y.-F., Li, X., et al. 2016, *ApJ*, 817, 64
- Zhu, W. W., Kaspi, V. M., McLaughlin, M. A., et al. 2011, *ApJ*, 734, 44